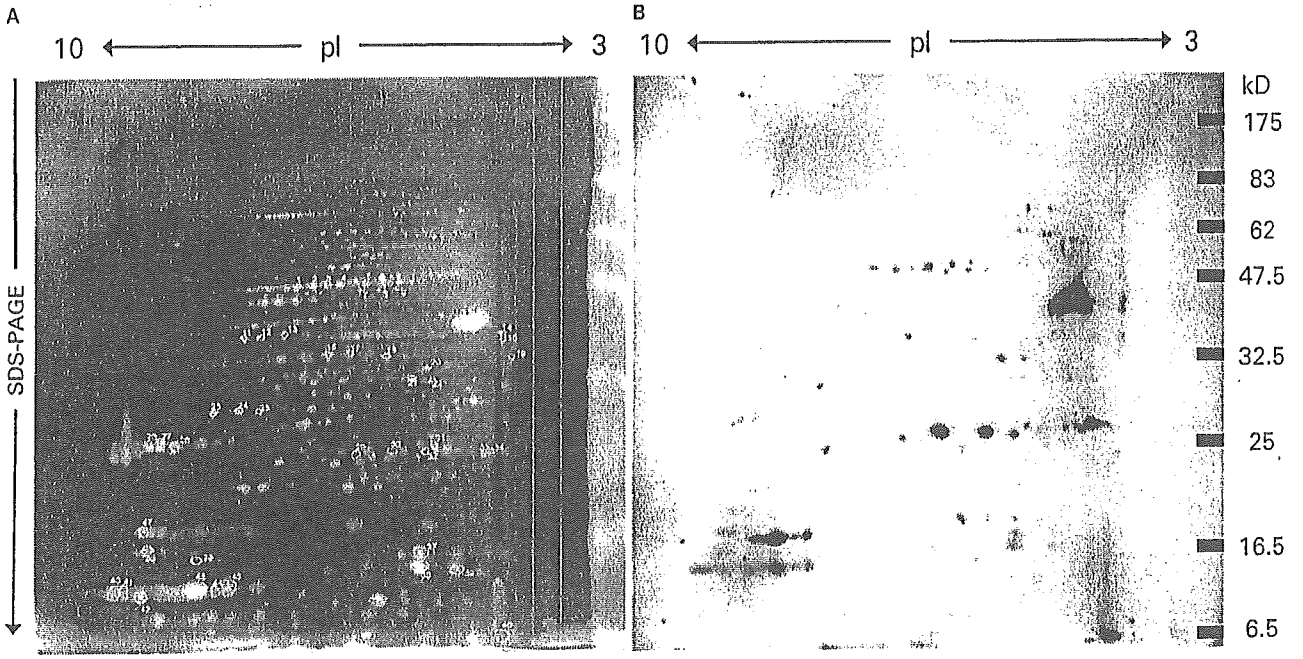

Fig. 1. Latex protein (**A**) and IgE-interactive protein (**B**) profiles on two-dimensional gels. Latex proteins extracted from NAL were first separated according to their isoelectric point (pI) on an immobilized pH gradient gel strip (pH 3–10, nonlinear). Second, the partially separated proteins were further resolved according to their molecular weight on a 10% acrylamide slab gel (SDS-PAGE). Two-dimensionally separated proteins were visualized by negative staining (**A**). IgE-interactive proteins submitted for subsequent in-gel digestion are highlighted and numbered (No. 1–47). For IgE immunoblotting (**B**), two-dimensionally separated proteins were transferred onto a membrane and treated by $NaIO_4$ for degradation of the possible carbohydrate structures. After blocking the unoccupied sites, the membrane was incubated in the pooled serum of 6 latex-sensitive patients. Spots of proteins that interacted with the IgE antibodies were then visualized by reaction with peroxidase-labeled anti-human IgE antibodies. The enzyme activity was recorded on a film using a chemiluminescent detection system. The migrating position and molecular weight of each marker protein are shown on the right side of the gel.

1. Mass error tolerance was set to plus or minus 0.5 D for PMF. In the MS/MS Ion Search mode, the mass error tolerance of a precursor ion was set to plus or minus 1.0 D, and plus or minus 0.5 D for the product ions. All the peptide masses mentioned in this article are monoisotopic masses. Sequentially homologous proteins from other organisms were searched using the Basic Local Alignment Search Tool (BLAST) search engine-based overall sequence of the top candidate picked up from the EST *(H. brasiliensis)* database.

Results

Two-Dimensional Immunoblotting of Latex Proteins

Proteins extracted from NAL were separated with two-dimensional gel electrophoresis. Its high resolution was visualized by negative staining of the gel (fig. 1A). More than 300 distinct protein spots, each with a different isoelectric point or molecular weight, were detected. This resolving power is far superior to the conventional SDS-PAGE or isoelectric focusing where proteins are separated one-dimensionally. IgE-interactive proteins were selectively detected by reaction with the pooled patients' serum following $NaIO_4$ treatment of a membrane binding the two-dimensionally separated proteins. $NaIO_4$ oxidatively degrades the carbohydrate structures of glycoproteins that tend to result in false-positive reactions of IgE antibodies by acting as monovalent antigens [17, 18]. Monovalent antigens cannot form a bridge-like structure of IgE antibodies attached to the specific receptor on a sensitized cell, and therefore they are believed not to provoke any allergic responses. We clearly detected more than 50 spots of proteins interacting with the IgE antibodies owing to the high resolving power of two-dimensional gel electrophoresis and the advanced sensitivity of the chemiluminescent detection system compared to conventional color-developing systems (fig. 1B). No significant spots of IgE-interactive proteins were detected when the pooled control serum was employed for immunoblotting (data not shown).

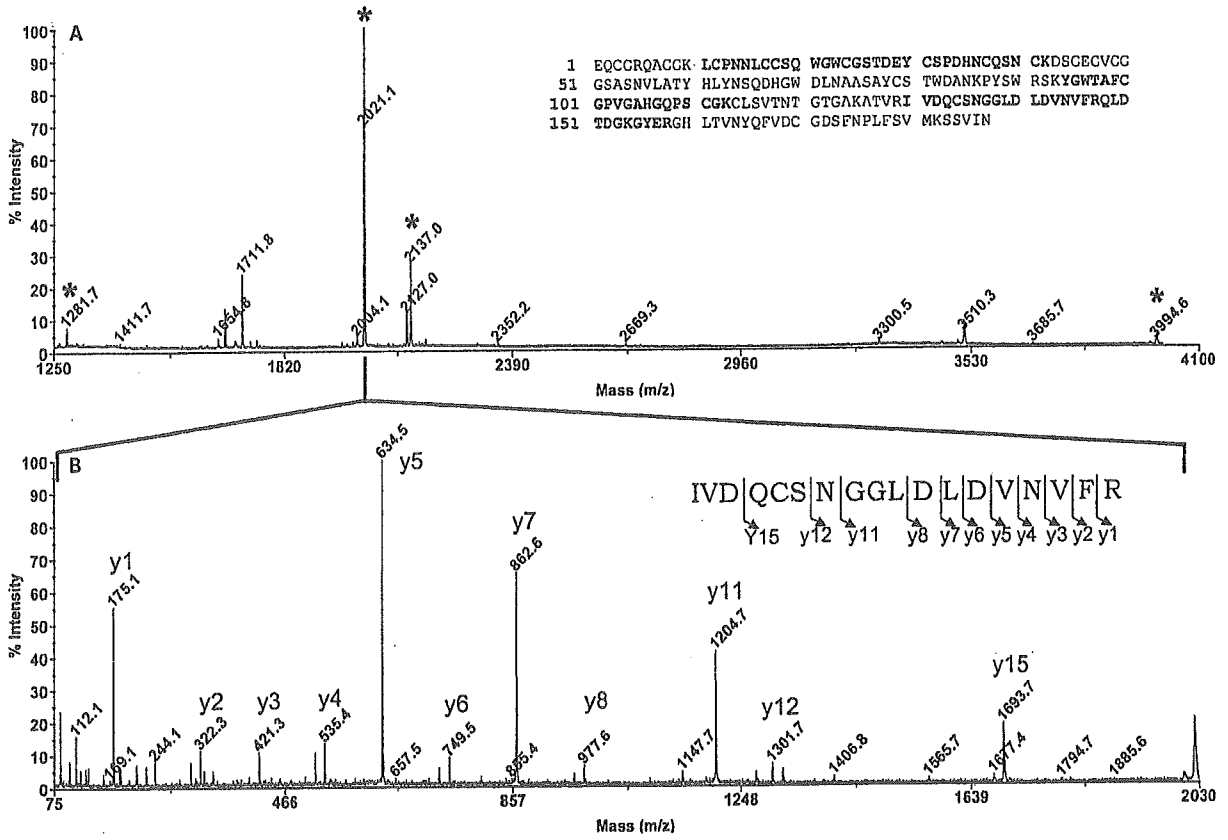

Fig. 2. Positive-ion reflectron MALDI-TOFMS spectrum (**A**) of tryptic peptides derived from an IgE-interactive protein (spot No. 38 in fig. 1A) and an MS/MS spectrum (**B**) of a prominently detected peptide ion (m/z 2021.1) on the peptide mass map. The spot of a putative allergen (No. 38) was cut out from a negatively stained two-dimensional gel (fig. 1A) and site-specifically cleaved by trypsin. The fragmented peptides were desalted using a reversed-phase microcolumn and spotted on a sample plate. α-Cyano-4-hydroxy cinnamic acid was used as a matrix for ionization. A peptide mass map (**A**) was used for PMF. This spectrum is a result of accumulation of 2,000 laser shots. The peptide ions assigned in the PMF search are labeled by asterisks, and their position is shown in boldface in the entire sequence of the top candidate (insert). The MS/MS spectrum (**B**) was recorded on the TOF-TOF mode of the instrument (4700 Proteomics Analyzer) and used for reading the PST. This MS/MS spectrum shows the accumulation of 5,000 laser shots. A partial sequence read from this spectrum is depicted as an insert with the name of the fragment ions (y series) detected. Based on a series of mass spectra including the ones shown in this figure, the original antigen (spot No. 38 in fig. 1A) was identified as a prohevein-related protein by database search (table 2).

In-Gel Digestion of Putative Allergens and Mass Spectrometry of Tryptic Peptides

Forty-seven spots of latex proteins that interacted with IgE antibodies from patients' sera were cut out from a two-dimensional gel (fig. 1A). With the help of the microtiter plate-based format of an in-gel digestion kit (Montage In-Gel Digest96 Kit), the putative allergens in the gel pieces were simultaneously digested by trypsin with less risk of keratin contamination. By adding *n*-octyl-β-*D*-glucoside to the digestion buffer, we could significantly improve the quality of mass spectra of fragmented peptides (fig. 2A). Desaltation of tryptic peptides using a reversed-phase microcolumn (ZipTip μC_{18}) was also helpful for improving the signal-to-noise ratio of the mass spectra (fig. 2A). We used a MALDI-TOF-TOF instrument for mass spectrometric analysis of tryptic peptides. Though the quality of MS/MS spectra is generally inferior to the spectra obtained on an electrospray ionization-based tandem mass spectrometer, the operation is less labor-intensive and very quick. The sensitivity of the mass spectrome-

Table 2. Summary of IgE-interactive proteins identified by allergenomics with a Mascot search

Spot No.	Name of the top candidate	Method used	Database used	Total score	Sequence coverage, %	Accession No.	Calculated Mr, kD	Calculated pI	Observed Mr, kD	Observed pI
1	UDP-glucose pyrophosphorylase	PST	NCBInr	46	2	gi|12585472	51.6	5.92	49.0	6.6
3	UDP-glucose pyrophosphorylase	PST	NCBInr	24	2	gi|12585472	51.6	5.92	49.0	6.4
4	UDP-glucose pyrophosphorylase	PST	NCBInr	58	6	gi|8099155	50.9	6.10	49.0	6.3
5	enolase 2 (Hev b 9)	PST	NCBInr	32	5	gi|14423687	48.1	5.92	49.0	6.3
7	enolase 1 (Hev b 9)	PMF	NCBInr	52	22	gi|14423688	48.0	5.57	47.5	6.0
	enolase 1 (Hev b 9)	PST	NCBInr	38	5	gi|14423688	48.0	5.57		
10	patatin-like latex allergen 2 (Hev b 7)	PMF	NCBInr	156	37	gi|7442023	43.0	5.00	40.0–43.5	4.6–5.5
	patatin-like latex allergen 1 (Hev b 7)	PST	NCBInr	68	13	gi|7442022	43.1	5.12		
21	isoflavone reductase[1]	PST	EST(latex)	201	15	gi|29054556	27.0	5.32	32.5	5.6
22	isoflavone reductase[1]	PST	EST(latex)	69	15	gi|29054556	27.0	5.32	32.5	5.4
26	hevamine A	PMF	NCBInr	151	54	gi|1311006	29.9	8.44	29.0	9.4
	hevamine A	PST	NCBInr	156	19	gi|1311006	29.9	8.44		
27	hevamine A	PMF	NCBInr	151	65	gi|1311006	29.9	8.44	29.0	9.3
	hevamine A	PST	NCBInr	240	32	gi|1311006	29.9	8.44		
28	hevamine A	PMF	NCBInr	137	54	gi|1311006	29.9	8.44	29.0	9.1
	hevamine A	PST	NCBInr	113	13	gi|1311006	29.9	8.44		
33	class I chitinase[1] (Hev b 11-related)	PST	EST(latex)	87	7	gi|29054149	23.5	8.28	26.5	4.2
34	class I chitinase[1] (Hev b 11-related)	PST	EST(latex)	121	15	gi|29054149	23.5	8.28	26.5	4.0
36	hevein precursor (Hev b 6-related)	PST	NCBInr	36	8	gi|123062	22.7	5.63	16.5	8.6
37	prohevein (Hev b 6)	PST	NCBInr	69	20	gi|2832430	20.9	5.64	17.0	5.6
38	prohevein (Hev b 6)	PMF	NCBInr	62	43	gi|2832430	20.9	5.64	15.0	5.6
	prohevein (Hev b 6)	PST	NCBInr	198	20	gi|2832430	20.9	5.64		
39	prohevein (Hev b 6)	PST	NCBInr	127	20	gi|2832430	20.9	5.64	15.0	5.3
40	rotamase	PST	SwissProt	21	6	Q39613	18.5	8.36	11.0	9.8
41	rotamase	PMF	SwissProt	38	27	Q39613	18.5	8.36	11.0	9.6
	rotamase	PST	NCBInr	50	6	gi|3334157	18.5	8.36		
42	rotamase	PST	NCBInr	98	8	gi|118104	18.6	8.91	10.5	9.3
43	prohevein (Hev b 6)	PMF	NCBInr	44	32	gi|2832430	20.9	5.64	11.0	8.7
	prohevein (Hev b 6)	PST	NCBInr	201	26	gi|2832430	20.9	5.64		
44	pseudo-hevein (Hev b 6-related)	PMF	NCBInr	49	33	gi|6562381	21.0	7.98	11.0	8.4
	prohevein (Hev b 6)	PST	NCBInr	114	20	gi|2832430	20.9	5.64		
45	pseudo-hevein (Hev b 6-related)	PMF	NCBInr	39	33	gi|6562381	21.0	7.98	11.0	8.0
	prohevein (Hev b 6)	PST	NCBInr	196	20	gi|2832430	20.9	5.64		
46	thioredoxin h	PST	NCBInr	48	13	gi|14485509	13.2	4.83	6.5	3.9
47	citrate-binding protein precursor	PST	NCBInr	72	10	gi|32363139	27.5	9.09	17.0	9.4

Mr = Molecular weight; pI = isoelectric point.
[1] Sequentially homologous protein was searched using BLAST.

try is also notable. We could easily obtain positive-ion peptide mass maps (fig. 2A) and MS/MS spectra of prominent ions (fig. 2B) from as small as several hundred femtomoles of tryptic peptides on a sample plate.

Identification of Putative Allergens by Database Search

Based on a peptide mass map of the tryptic peptides and MS/MS spectra of the intense peptide ions, the proteins in question were identified by database search. The identified putative allergens are listed in table 2, with the total score and sequence coverage rate showing the certainty of the protein candidate. Thanks to the high resolution of two-dimensional gel electrophoresis and the remarkable sensitivity of MALDI-TOFMS, we could identify five new allergen candidates (UDP-glucose pyrophosphorylase, isoflavone reductase, rotamase, thioredoxin and citrate-binding protein) and five previously reported latex allergens or their relatives (Hev b 9, Hev b 7, Hev b 11, Hev b 6 and hevamine) without isolating each protein

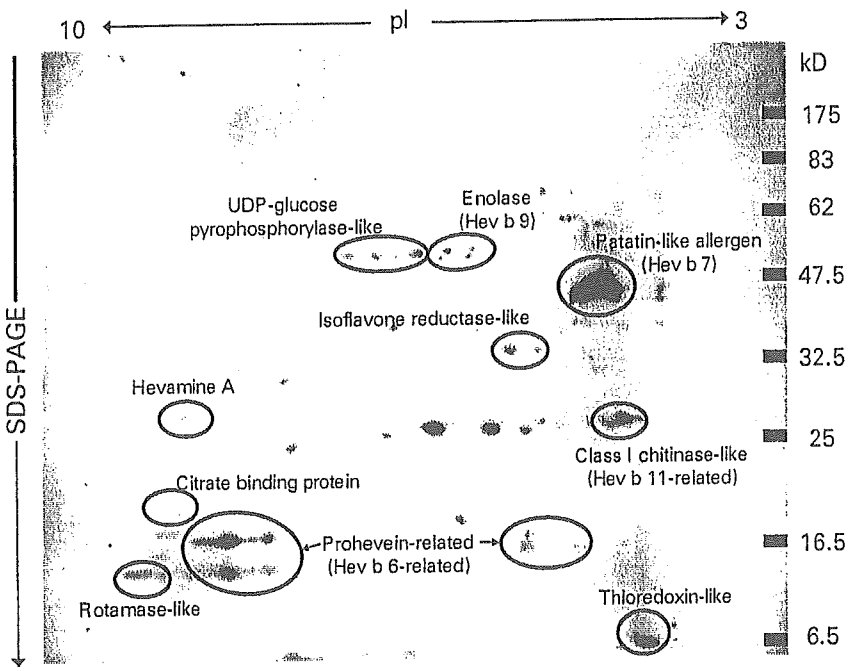

Fig. 3. Putative latex allergens identified by a proteomic strategy. The names of the top candidates are shown on an IgE immunoblot (same as in fig. 1B). Spots enclosed by an ellipse are IgE-interactive proteins assigned to the same or closely related entries (isoallergens) by database search. More information on each antigenic protein is presented in table 2.

(table 2, fig. 3). A few allergens were identified by database search with the PMF mode of Mascot, but the searching based on PST was much more powerful for protein identification. From the MS/MS spectra of tryptic peptides derived from a protein, we could obtain information on the partial sequences (fig. 2B) that would be valuable for designing the oligonucleotide probes as well as for the database search. The BLAST search was also effective in finding a protein candidate that is sequentially comparable to a DNA fragment registered in the EST database *(H. brasiliensis)*. The entire protocol, from two-dimensional gel electrophoresis to the database search, was accomplished quickly. We were able to analyze about 50 IgE-interactive latex proteins within 1 week.

Discussion

In this study, we evaluated the usefulness of a proteomic strategy for analyzing putative allergens (allergenomics) through application to latex proteins. Latex proteins were first separated two-dimensionally according to their isoelectric point and molecular weight under denaturing conditions. Two-dimensional gel electrophoresis appeared to be remarkably superior to SDS-PAGE with regard to its high resolution. In conventional SDS-PAGE, proteins were separated based solely on their molecular weight under a denaturing condition. Therefore, a seemingly single band on an SDS-PAGE gel frequently contains several protein entities. This poor resolution might bring about erroneous identification of IgE-interactive proteins. Additionally, faint structural differences of isoallergens are hardly reflected on SDS-PAGE gel and subsequent IgE immunoblot. In contrast, we can detect slight structural differences of isoallergens as distinct spots on a two-dimensional gel and subsequent IgE immunoblot. Hev b 7 isoallergens are one such example (fig. 3, table 2, spot No. 10). Historically, the reproducibility of two-dimensional gel electrophoresis has been a critical problem in applying this technique to research of complex protein mixtures. However, the appearance of commercially available immobilized pH gradient gels has solved a large part of this difficulty. The effectiveness of two-dimensional gel electrophoresis for analysis of allergenic proteins has already been demonstrated in previous studies [19–23]. Nevertheless, this technique has not attracted the attention of many researchers, due to the lack of a convenient identification method for the resolved proteins. N-terminal sequence analysis of a purified protein has been the first choice for identification [10, 20], but this technique is time-consuming and requires a relatively large quantity of purified sample. Putative allergens avail-

able only in minute amounts were therefore not readily amenable to this approach.

As the sequence data of proteins and genes accumulate in databases, the situation is changing. Candidate proteins are becoming easier to identify after site-specific fragmentation and mass spectrometric analysis of the component peptides [9, 10]. Mass spectrometry is so sensitive that we can analyze putative allergens on quantities as small as the nanogram or several hundred-femtomole level. Intensive research of such a small quantity of proteins was impossible with traditional Edman degradation-based N-terminal sequencing. The speed of mass spectrometric analysis is also advantageous. We can obtain thousands of mass spectra and MS/MS spectra within a day using a MALDI-TOFMS instrument. Semiautomated analysis of fragmented peptides from spotting on a sample plate to output of the mass spectra is also possible. By combining with high-resolution two-dimensional gel electrophoresis, the mass spectrometric approach will certainly become the most powerful means for fast and exhaustive analysis of IgE-interactive proteins [24].

The efficiency of allergenomics was substantiated in this study through the analysis of latex proteins. We were able to identify five new allergen candidates as well as five previously reported allergens without any difficulties (fig. 3, table 2). The required starting material was less than 1 mg. In addition, the entire analysis was completed within 1 week; two-dimensional gel electrophoresis and subsequent IgE immunoblotting usually takes not more than 5 days. Referring to the immunoblotting result with pooled patients' serum, IgE-interactive proteins were cut out from a two-dimensional gel and digested by trypsin overnight. A more rapid digestion protocol for proteins is also applicable [25]. The proteins in question were identified the next day from mass spectrometric analysis of the resulting fragments and subsequent database search. These analytical steps for each IgE-interactive protein proceed in parallel with the help of a microtiter plate-based tryptic digestion regime. In this way, allergenomics was concretely verified as a quick and effective strategy for exhaustive analysis of IgE-interactive proteins from various species.

We should point out at this stage that IgE-interactive proteins or antigens identified with allergenomics are just putative allergens or allergen candidates. IgE-binding activity of a protein is one of the prerequisites for it to be an allergen and does not necessary indicate its actual allergenicity. Some IgE-interactive proteins are indeed asymptomatic but others are symptomatic [17, 18]. Therefore, the actual allergenicity of putative allergens must finally be confirmed with other techniques like SPT or histamine release test. This situation is common to almost all the allergen identification procedures reported to date where allergen candidates are screened based on their IgE-binding activity.

Even though allergenomics is very promising, as already illustrated, some of the latex antigens were not identified by database search, as shown in figure 3, despite their clear detection in IgE immunoblotting. There are two possible reasons for this failure. One possibility is that the quantity of IgE-interactive protein was too small to gain meaningful data regardless of the high sensitivity of the mass spectrometry. Another possibility is that data on the sequence of the antigen in question had not been registered in the databases used. The genome of the rubber tree *(H. brasiliensis)* has not been sequenced thoroughly. Therefore, we cannot identify some of the latex proteins by the proteomic strategy in principle. If we analyze proteins from rice or *Arabidopsis,* this is not the case because the genome projects of these species have already been finished. Even when the sequence of an IgE-interactive protein is not included in databases, we can search sequentially homologous proteins from other species using the partial sequences of tryptic peptides or cDNA fragments. Moreover, the gene coding the putative allergen can be fully sequenced by cloning the corresponding cDNA using oligonucleotide probes designed from the revealed partial sequences. These prospects for further research also suggest the versatility of allergenomics.

Acknowledgement

This study was supported in part by a grant for Research on Advanced Medical Technology provided by the Ministry of Health, Labor and Welfare, Japan.

References

1 Ebo DG, Stevens WJ: IgE-mediated natural rubber latex allergy: An update. Acta Clin Belg 2002;57:58–70.
2 Yagami T, Sato M, Nakamura A, Komiyama T, Kitagawa K, Akasawa A, Ikezawa Z: Plant defense-related enzymes as latex antigens. J Allergy Clin Immunol 1998;101:379–385.
3 Yagami T: Plant defense-related proteins and latex allergy. Environ Dermatol 1998;5(suppl 2):31–39.
4 Yagami T: Defense-related proteins as families of cross-reactive plant allergens. Recent Res Dev Allergy Clin Immunol 2000;1:41–64.
5 Yagami T: Allergies to cross-reactive plant proteins: Latex-fruit syndrome is comparable with pollen-food allergy syndrome. Int Arch Allergy Immunol 2002;128:271–279.
6 Yagami T: Features and mode of action of cross-reactive plant allergens relevant to latex-fruit syndrome. Food Agric Immunol 2002;14: 241–253.
7 Wagner S, Breiteneder H: The latex-fruit syndrome. Biochem Soc Trans 2002;30:935–940.
8 Blanco C: Latex-fruit syndrome. Curr Allergy Asthma Rep 2003;3:47–53.
9 Peng J, Gygi SP: Proteomics: The move to mixtures. J Mass Spectrom 2001;36:1083–1091.
10 Tichá M, Pacáková V, Štulík K: Proteomics of allergens. J Chromatogr B Analyt Technol Biomed Life Sci 2002;771:343–353.
11 Raftery MJ, Saldanha RG, Geczy CL, Kumar RK: Mass spectrometric analysis of electrophoretically separated allergens and proteases in grass pollen diffusates. Respir Res 2003;4:10.
12 Petersen A: Two-dimensional electrophoresis replica blotting: A valuable technique for the immunological and biochemical characterization of single components of complex extracts. Proteomics 2003;3:1206–1214.
13 Dreborg S: Skin tests in the diagnosis of food allergy. Pediatr Allergy Immunol 1995;6(suppl 8):38–43.
14 Katayama H, Satoh K, Takeuchi M, Deguchi-Tawarada M, Oda Y, Nagasu T: Optimization of in-gel protein digestion system in combination with thin-gel separation and negative staining in 96-well plate format. Rapid Commun Mass Spectrom 2003;17:1071–1078.
15 Katayama H, Nagasu T, Oda Y: Improvement of in-gel digestion protocol for peptide mass fingerprinting by matrix-assisted laser desorption/ionization time-of-flight mass spectrometry. Rapid Commun Mass Spectrom 2001;15: 1416–1421.
16 Medzihradszky KF, Campbell JM, Baldwin MA, Falick AM, Juhasz P, Vestal ML, Burlingame AL: The characteristics of peptide collision-induced dissociation using a high-performance MALDI-TOF/TOF tandem mass spectrometer. Anal Chem 2000;72:552–558.
17 Yagami T, Osuna H, Kouno M, Haishima Y, Nakamura A, Ikezawa Z: Significance of carbohydrate epitopes in a latex allergen with β-1,3-glucanase activity. Int Arch Allergy Immunol 2002;129:27–37.
18 Van Ree R: Carbohydrate epitopes and their relevance for the diagnosis and treatment of allergic diseases. Int Arch Allergy Immunol 2002;129:189–197.
19 Kurup VP, Alenius H, Kelly KJ, Castillo L, Fink JN: A two-dimensional electrophoretic analysis of latex peptides reacting with IgE and IgG antibodies from patients with latex allergy. Int Arch Allergy Immunol 1996;109:58–67.
20 Posch A, Chen Z, Wheeler C, Dunn MJ, Raulf-Heimsoth M, Baur X: Characterization and identification of latex allergens by two-dimensional electrophoresis and protein microsequencing. J Allergy Clin Immunol 1997;99: 385–395.
21 Duong PT, Chang FN: A simple method for assigning multiple immunogens to their protein on a two-dimensional blot and its application to asthma-causing allergens. Electrophoresis 2001;22:2098–2102.
22 Beyer K, Bardina L, Grishina G, Sampson HA: Identification of sesame seed allergens by 2-dimensional proteomics and Edman sequencing: Seed storage proteins as common food allergens. J Allergy Clin Immunol 2002;110: 154–159.
23 Beyer K, Grishina G, Bardina L, Grishin A, Sampson HA: Identification of an 11S globulin as a major hazelnut food allergen in hazelnut-induced systemic reactions. J Allergy Clin Immunol 2002;110:517–523.
24 Yu CJ, Lin YF, Chiang BL, Chow LP: Proteomics and immunological analysis of a novel shrimp allergen, Pen m 2. J Immunol 2003; 170:445–453.
25 Russell WK, Park ZY, Russell DH: Proteolysis in mixed organic-aqueous solvent systems: Applications for peptide mass mapping using mass spectrometry. Anal Chem 2001;73:2682–2685.

CHANGE OF THE CELLULAR FUNCTION BY CONNEXIN GENE TRANSFECTION IN A HEPATOMA CELL LINE

Jun YANG[1], Akira ICHIKAWA[2], Toshie TSUCHIYA[1]
[1]*Division of Medical Devices, National Institute of Health Sciences, 1-18-1 Kamiyoga, Setagaya-ku, Tokyo 158-8501, Japan*
[2]*Department of Applied Biology, Faculty of Textile Science, Kyoto Institute of Technology, Goshokaido-cho, Matsugasaki, Sakyo-ku, Kyoto 606-8585,Japan*

Abstract

Connexin 32 (Cx32) is the main gap junction protein in hepatocytes and plays an important role in the regulation of liver gap junctional communication (GJIC). In this study, the human Cx32 gene was transfected in a hepatoma cell line (HepG2) that is aberrant expression of Cx32 and deficient in GJIC. Cx32-transfected HepG2 showed the increased GJIC comparing with HepG2 and the vector-transfected HepG2. Furthermore, the liver functions of ammonia removal activity of HepG2 were remarkably enhanced with Cx32 gene transfection. It may be expected to improve the cellular functions of the hepatoma cell line by Cx32 gene transfection and serve to develop an efficacious bioartificial liver.

Introduction

A cell-based biohybrid artificial liver (BAL) is a promising approach to support patients with acute liver failure[1]. To overcome worldwide shortage of donor organs and avoid xenozoonosis risk, a hepatoma cell line HepG2 derived form the human-origin cell has growth characteristic and are less severe antigenecity, and then has already been used for developing the BAL[2]. Although HepG2 keeps liver-specific functions well among hepatoma cell lines, the activities of the liver-specific functions in HepG2 were far lower comparing with these of primary hepatocytes[3]. On the other hand, gap junction intercellular communication (GJIC) is considered to play an essential role in the control of proliferation, differentiation and homeostasis of various cells. In the liver, hepatocytes are coupled to each others by gap junctions and GJIC is necessary for liver homeostasis growth control and signal transfer, especially related to glycogen

K. Yagasaki et al. (eds.), Animal Cell Technology: Basic & Applied Aspects, Volume13, 293-297.

mobilization and neoplastic transformation[4]. However, HepG2 is aberrant expression of connexin protein and is deficient in GJIC. In the liver, connexin32 (Cx32) is the major gap junction protein expressed in hepatocytes, therefore, the aim of this study is focused on enhancing GJIC and improving liver-specific functions of HepG2 by Cx32 gene transfection.

Key word: Bioartificial liver, Connexin, Hepatoma cell

2. Materials and Methods

2.1. Cell culture

The human hepatoma cell lines HepG2 from the Riken cell bank (Tokyo, Japan) was cultured at 37℃ under 5% CO_2 / 95% humidified air using Minimum Essential Medium (MEM) (Nissui Pharmaceutical Co., Ltd., Tokyo, Japan) containing 0.1mM non-essential amino acids (NEAA) (Gibco), 10% fetal bovine serum (FBS) (Intergen Co., NY.) and 100U/ml Penicillin-Streptomycin (Gibco).

2.2. Plasmid construction and transfection

The connexin gene fragments amplified by polymerase chain reaction were isolated and inserted into the pTARGET™ mammalian expression system. HepG2 cells were transfected with the Cx/pTARGET™ plasmid DNA using FuGENE6 transfection reagent according to manufacturer's instruction with minor modification, cells transfected with empty vector as a control. After continuously culturing for two days, transfectants were selected by adding geneticin (Life Technologies, Inc., Frederick, MD) in the culture medium for one week. Individual transfected clones were prepared by limiting dilution cloning in 96-well plates, and then cultured as same as the HepG2.

2.3. Immunocytochemical stainings

Immunocytochemical staining of Cx32 protein was performed using the VECTASTAIN ABC kit in manufacturer's instruction with some modification. Briefly, cells grown on the glass cover slips were fixed in cold pure acetone for 5 min. The acetone-fixed specimens were blocked in diluted normal blocking serum in Dulbecco's phosphate buffered saline (PBS) at room temperature for 30min, and incubated with polyclonal rabbit anti-connexin32 (Zymed Laboratories Inc., San Francisco, CA) over night at 4 ℃ . Protein-antibody complexes were visualized by the biotin/streptoavidin/peroxidase method with diaminobenzidine tetrahydrochloride (DAB) as the chromogen (Vextor Laboratories, Burlingame, USA). All slides were viewed with a Nikon microscope (Nikon, Japan).

2.4. Scrape-loading dye transfer (SLDT) assay for measurement of GJIC

The SLDT technique was adapted after the method of El-Fouly et al. [5]. Briefly, when the cells grew into confluent monolayer cells in 35-cm dishes, cell dishes were loaded with 0.05% Lucifer Yellow (Molecular Probes, Eugene, OR, USA) in PBS (+) solution and were scraped immediately with a sharp blade after rinsing with PBS (+). Then incubating for 5 min at 37℃, cells were washed with PBS (+) and monitored using fluorescence microscope. The distance of the dye spreading was measured from the cell layer at the scrape to the edge of the dye front that was visually detectable.

2.5. Liver-specific function assay

The functions of the HepG2 and Cx32 transfected cells were evaluated by measuring ammonia removal and albumin secretion. For the ammonia removal activities of these cells, the cells were cultured in MEM medium with 5mM ammonium chloride. After the exchange of the medium containing ammonium, the concentration of ammonia in the medium was measured at 0 and 24hrs, respectively, using the indophenol method (an ammonia assay kit, Wako Pure Chem., Japan).

2.6. Statistical analysis

Student's t-test was used to compare the samples. Statisticall significance was represented by $p<0.05$. Date were indicated as the mean±S.D (Standard Daviation). Three cultures were run for each case, and all experiments were repeated at least twice.

3. Results and Discussion

3.1. Functional GJIC in HepG2 enhanced by Cx32 gene transfection

HepG2 cells were transfected with Cx32/pTARGET™ plasmid DNA using FuGENE6 transfection reagent, and the transfectants were obtained by selection with geneticin. Enhanced expression of Cx32 mRNA was confirmed by RT-PCR (date not shown). The abilities of GJIC in Cx32 plasmid DNA transfectants were investigated by the scrape-loading dye transfer technique. Lucifer yellow, a molecular probe with low molecular weight, can diffuses in the neighboring cells through the gap junction, but not transmits from intact plasma membranes. Therefore, the transfer distances of lucifer yellow reflect the functional GJIC in the cells, and the longer distance shows the higher functional GJIC in the cells. The transfer distance of lucifer yellow in Cx32 gene transfected cells was longer than those of HepG2 and empty vector transfected cells. Thus, the distance in Cx32 gene transfected cells was 2.8 times and 2 times as long as that of HepG2 and empty vector transfected cells, respectively. It could be concluded

that the functional GJIC in HepG2 was significantly enhanced by the Cx32 gene transfection.

3.2. Localization of Cx32 protein before and after Cx32 gene transfection

In order to confirm the contribution of Cx32 proteins for the formation of functional GJIC after the Cx32 gene transfection, the localizations of Cx32 protein in the cells were further observed by immunocytochemical staining (Fig.1). The results demonstrated that the Cx32 protein expressed in HepG2, Cx32 gene transfected cells

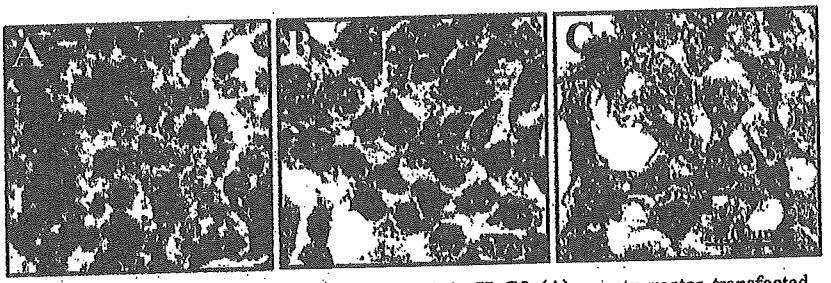

Fig.1. Immunocytochemical staining for Cx32 in HeG2 (A), empty vector transfected cells (B) and Cx32 gene transfected cells (C).

and empty vector transfected cells, but the localizations of Cx32 protein were obviously different among them. Thus, the Cx32 protein was localized in the cell borders and formed many small gap junction plaques in the neighboring cells transfected with Cx32 gene (Fig.1.C), however, the Cx32 protein was limited in the cytoplasm and hardly detected the gap junction plaques in the HepG2 (Fig.1.A) and empty vector transfected cells (Fig.1.B). Furthermore, the morphologies of the cells showed that Cx32 gene transfected cells grew as a monolayer with the spreading cell shape, whereas the HepG2 grew as the clusters with the spherical cell shape. Although the precise role of the cellular morphology in gap junctional channel formation between the cells is not clear at the present, the results in our study could be concluded that the traffic of Cx32 protein to the cell membrane in HepG2 was enhanced by Cx32 gene transfection and then increased the GJIC in Cx32 gene transfected cells.

3.3. Liver-specific function in HepG2 improved by Cx32 gene transfection

For determining the effect of Cx32 gene transfection on the liver-specific function in HepG2, the ammonia removal activity were continuously monitored in the HepG2, empty vector transfected cells and Cx32 gene transfected cells, respectively. Ammonia clearance, which represents the detoxification potentiality of liver, was significantly higher in the Cx32 gene transfected cells than HepG2 and empty vector transfected cells

during the 14 days. These results showed that the ammoniun metabolic activity in HepG2 related with the functional gap junctional channel composed of Cx32 proteins. It was considered that the small molecular ammonium was effectively eliminated through the gap junctional channels improved by Cx32 gene transfection in HepG2.

In conclusion, transfection of Cx32 gene increased the functional GJIC in HepG2 and enhance the activity of detoxification in the Cx32 gene transfected HepG2. It may be expected to improve the cellular function of the hepatoma cell line by Cx32 gene transfection and serve to develop an excellent biohybrid-artificial liver.

References:

1. Sussman NL, Gislason GT, Conlin CA, Kelly JH (1994) The hepatix extracorporeal liver assist device-initial clinical experience. *Artif Oegans* 18:390-396.
2. Yamashita Y, Shimada M, Tsujita E, Tanaka S, Ijima H, Nakazawa K, Sakiyama R, Fukuda J, Ueda T, Funatsu K, Sugimachi K. (2001) Polyurethane foam/spheroid culture system using human hepatoblastoma cell line (HepG2) as a possible new hybrid artificial liver. *Cell Transplantation* 10:717-722.
3. Takagi M, Fukuda N, Yoshida T. (1997) Comparison of different hepatocyte cell lines for use in a hybrid artificial liver model. *Cytotechnology* 24:39-45.
4. Marie PP, Rosanne MT, Martha JF, Robert DB, Randall JR. (2000) Liver cell-specific transcriptional regulation of connexin 32. *Biochimica et Biophysica Acta* 1491:107-122.
5. El-Fouly MH, Trosko JE, Chang CC. (1987) Scrape-loading and transfer: Arapid and simple technique to study gap junctional intercellular communication. *Exp. Cell Res.* 168:422-430.

Available online at www.sciencedirect.com
SCIENCE DIRECT®
Tetrahedron Letters
Tetrahedron Letters 45 (2004) 527–529

Synthesis of C_{60} derivatives for photoaffinity labeling

Eiji Okada,[a,b] Yuka Komazawa,[a,b] Masaaki Kurihara,[a] Hideshi Inoue,[b] Naoki Miyata,[a] Haruhiro Okuda,[a] Toshie Tsuchiya[a] and Yoko Yamakoshi[a,*]

[a]*National Institute of Health Sciences, 1-18-1 Kamiyoga, Setagaya, Tokyo 158-8501, Japan*
[b]*School of Life Sciences, Tokyo University of Pharmacy and Life Sciences, 143201 Horinouchi, Hachioji, Tokyo 192-03, Japan*

Received 9 October 2003; accepted 31 October 2003

Abstract—In order to study the interaction of fullerenes with biological molecules, a novel photoaffinity labeling agent derived from C_{60} was designed and synthesized. As photosensitive functional groups, azide group, and aziridine group are utilized. A convenient synthetic route via fulleropyrrolidine **2** was employed to obtain compounds labeling agents **5** and **9**.

The biological activities of fullerenes have attracted considerable attention due to their potential medicinal applications.[1-3] Their novel and unexploited properties stem from their bulky hydrophobic shape and their photosensitivity[4-7] and radical-generating[8-11]/-quenching[12,13] activities enabled by highly conjugated π-electron system.

As a most remarkable activity, direct inhibition of enzymes by C_{60} has been reported. The first example, HIV-1 protease inhibition by a water soluble fullerene derivative, was reported in 1993[14-16] by Wudl, Wilkins, et al. Independently, Toniollo et al. has reported C_{60}-peptide conjugates and identified activity of these compounds against HIV-1 protease and chemotatic activity against human monocytes.[17] Separately, we have developed new procedures for solubilizing C_{60} in water[18] and assayed unfunctionalized C_{60} for direct enzymatic inhibtion. These studies led to the discovery that aqueous solutions of C_{60} inhibit glutathione-*S*-transferase (GST).[19]

The ability of C_{60}, which is large (7 Å id) hydrophobic molecules, to bind to biological compounds, was initially surprising and several groups have attempted to identify and calculate the binding sites. Based on a computer simulated docking study, Wudl, Wilkins, et al. speculated that the C_{60} core was enclosed in the cylindrical active site, which consists primarily of hydrophobic amino acid residues, of HIV-1 protease. In our own work, we calculated that C_{60} binds to GST at a cleft between two subunits of the enzyme, although the specific residues, which make up the active site are unclear.[20]

In order to clarify the more detailed binding site of C_{60}, two solutions are possible as follows. One is to isolate pure enzyme–fullerene complex and determine the structure by NMR or crystallographic methods. Another potential method for identifying the active site area is photoaffinity labeling, which is particularly useful for identifying the active site in solution under physiological conditions.

We now report the design and synthesis of the first C_{60}-derived photoaffinity labeling reagents. Our synthetic route to photoaffinity reagents **5** and **9** provide a concise, flexible route to fullerenes functionalized with photoreactive pendant groups such as phenylazide and phenyldiazirine, which generate aryl nitrene and aryl carbene, respectively (Eqs. 1 and 2).[21]

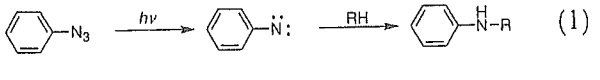

(1)

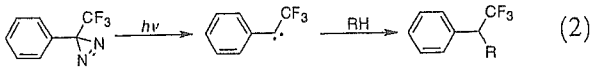

(2)

In order to develop an efficient and flexible synthetic method, which would allow the late-stage introduction of a variety of photoaffinity labels, we chose to utilize dimethylfulleropyrrolidine (**2**). This C_{60} derivative

* Corresponding author. Tel.: +81-3-3700-1141; fax: +81-3-3707-6950; e-mail addresses: yamakosh@nihs.go.jp, yamakoshi@chem.ucsb.edu

0040-4039/$ - see front matter © 2003 Published by Elsevier Ltd.
doi:10.1016/j.tetlet.2003.10.212

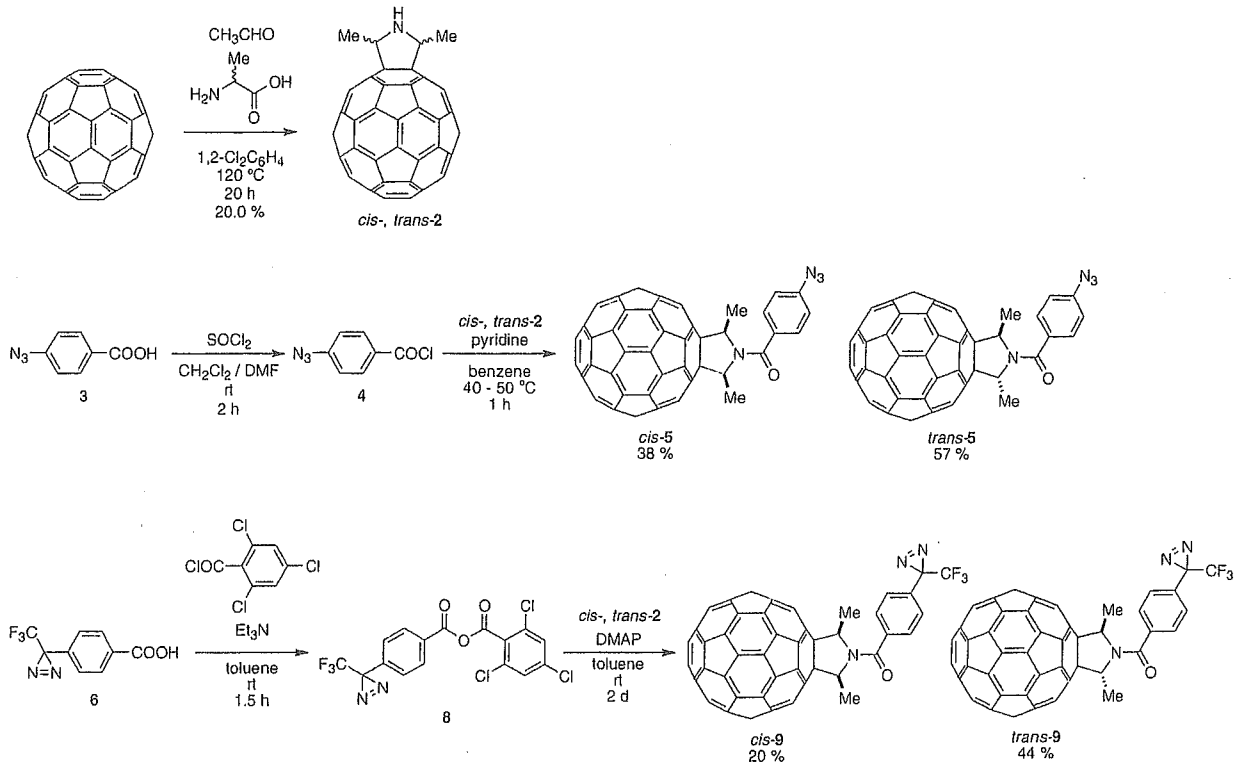

Scheme 1. Synthesis of C_{60} derivatives with phenylazide (**5**) and phenylaziridine (**9**) group.

is readily prepared by the method of Prato and co-workers[22] and Wilson and co-workers.[23,24] This route provides a convenient approach to C_{60} derivatives with a secondary amine as an ideal site for the incorporation of further functionalization.

The synthesis of phenylazide derivative of fullerene was achieved as shown in Scheme 1. Dimethyl fulleropyrrolidine **2** (*cis*- and *trans*-mixture) was prepared by 1,3-dipolar cycloaddition[25] and then acylated with acid chloride **4** to give *cis*- and *trans*-C_{60}-phenylazide derivatives **5**, which can be easily separated by silica gel column chromatography.[26]

To synthesize the C_{60}-phenyldiazirine derivative **9**, we first attempted the reaction of fulleropyrrolidine **2** with an acid chloride, but this reaction did not give useful amounts of the desired product. Despite attempts to activate the acyl moiety by a succinimide group using 4-(3-trifluoromethylazirino)benzoic succinimide, product formation was not observed. In sharp contrast, however, the use of Yamaguchi reagent **8** to couple **6** and **2** gave good yields of *cis*- and *trans*-C_{60}-phenyldiazirine derivatives **9**.[27] These stereoisomers are readily separated by silica gel chromatography. Compounds **5** and **9** were characterized by spectroscopic methods.[28] The *cis*- and *trans*-stereochemistry of each compounds were determined according to the reported studies.[23,24]

In addition to the potential utility of fullerene-derived photoaffinity labels for elucidating the active site of C_{60} binding to enzymes such as GST and HIV-1 protease, the ability to selectively tag a protein or enzyme with fullerene may offer a new approach to the detection of biological molecules with high sensitivity. For example, an acidic isozyme of GST is specified as cancer expressing marker in liver cancers.[29,30] The ability to selectively tag such diagnostic enzymes with C_{60}, which has unique and useful chemical and photophysical properties, may offer a novel and rapid detection method for identifying trace amounts of enzyme present in a biological sample. These and other applications of the reported photoaffinity labeling reagents currently in progress.

In conclusion, we have described a concise and flexible route to fullerene-derived photoaffinity labels with potential utility in enzyme tagging and the elucidation of the binding sites of protein to C_{60}.

Acknowledgements

We are grateful to thank Dr. Nobuo Ikota in National Institute of Radiological Sciences for his fruitful discussions on the synthetic methodologies. We also thank Prof. Dr. Jeffrey W. Bode at University of California Santa Barbara for his advice. This research was supported in part by Grant-in-Aid for Research on Advanced Medical Technology from Ministry of Labor, Health and Welfare (TT, YY), Grant-in-Aid for Encouragement of Young Scientists from Ministry of Education, Science, Sports and Culture, Japan [Nos. 08772153 (YY), 09772037 (YY) and 13771418 (YY)], Grant-in-Aid for young researchers from Ministry of Health and Welfare (YY) and Grant-in-Aid for young researchers from Human Science Foundation (YY).

References and Notes

1. Jensen, A. W.; Wilson, S. R.; Schuster, D. I. *Bioorg. Med. Chem.* **1996**, *4*, 767–786.
2. Da Ros, T.; Prato, M. *Chem. Commun.* **1999**, 663–669.
3. Wilson, S. R. In *Fullerenes: Chemistry, Physics and Technology*; Kadish, K. M., Ruoff, R. S., Eds.; A John Wiley and Sons: New York, 2000; pp 437–466.
4. Foote, C. S. In *Physics and Chemistry of the Fullerene*; Prassodes, K., Ed.; Kluwer Academic: Dordrecht, 1994; pp 79–96.
5. Foote, C. S. *Top. Curr. Chem.* **1994**, *169*, 347–363.
6. Guldi, D. M.; Prato, M. *Acc. Chem. Res.* **2000**, *33*, 695–703.
7. Guldi, D. M.; Kamat, P. V. In *Fullerenes: Chemistry, Physics and Technology*; Kadish, K. M., Ruoff, R. S., Eds.; A John Wiley and Sons: New York, 2000; pp 225–282.
8. Krusic, P. J.; Wasserman, E.; Parkinson, B. A.; Malone, B.; Holler, E. R., Jr.; Keizer, P. N.; Morton, J. R.; Preston, K. F. *J. Am. Chem. Soc.* **1991**, *114*, 6274–6275.
9. Arbogast, J. W.; Foote, C. S.; Kao, M. *J. Am. Chem. Soc.* **1992**, *114*, 2277–2279.
10. Brezova, V.; Stasko, A.; Rapta, P.; Domschke, G.; Bartl, A.; Dunch, L. *J. Phys. Chem.* **1995**, *99*, 16234–16241.
11. Yamakoshi, Y.; Sueyoshi, S.; Fukuhara, K.; Miyata, N.; Masumizu, T.; Kohno, M. *J. Am. Chem. Soc.* **1998**, *120*, 12363–12364.
12. Chiang, L.; Lu, F.-J.; Lin, J.-T. *J. Chem. Soc., Chem. Commun.* **1995**, 1283–1284.
13. Okuda, K.; Mashino, T.; Hirobe, M. *Bioorg. Med. Chem. Lett.* **1994**, *6*, 539.
14. Friedman, S. H.; DeCamp, D. L.; Sijbesma, R. P.; Srdanov, G.; Wudl, F.; Kenyon, G. L. *J. Am. Chem. Soc.* **1993**, *115*, 6506–6509.
15. Sijbesma, R. P.; Srdanov, G.; Wudl, F.; Castoro, J. A.; Wilkins, C.; Friedman, S. H.; DeCamp, D. L.; Kenyon, G. L. *J. Am. Chem. Soc.* **1993**, *115*, 6510–6512.
16. Schinazi, R. F.; Sijbesma, R. P.; Srdanov, G.; Hill, C. L.; Wudl, F. *Antimicrob. Agents Chemother.* **1993**, *37*, 1707–1710.
17. Toniolo, C.; Bianco, A.; Maggini, M.; Scorrano, G.; Prato, M.; Marastoni, M.; Tomatis, R.; Spisani, S.; Palu, R.; Blair, D. E. *J. Med. Chem.* **1994**, *37*, 4558–4562.
18. Yamakoshi, Y.; Yagami, T.; Fukuhara, K.; Sueyoshi, S.; Miyara, N. *J. Chem. Soc., Chem. Commun.* **1994**, 517–518.
19. Iwata, N.; Mukai, T.; Yamakoshi, Y.; Hara, S.; Yanase, Y.; Shoji, M.; Endo, T.; Miyata, N. *Fullerene Sci. Technol.* **1998**, *6*, 213–226.
20. Miyata, N.; Yamakoshi, Y.; Inoue, H.; Kojima, M.; Takahashi, K.; Iwata, N. In *Fullerenes: Recent Advances in the Chemistry and Physics of Fullerenes and Related Materials*; Kadish, K. M., Ruoff, R. S., Eds.; The Electrochemical Society, Inc.: Pennington, NJ, 1998; Vol. 6, pp 1227–1235.
21. Fleming, S. A. *Tetrahedron* **1995**, *46*, 12479–12520.
22. Maggini, M.; Scorrano, G.; Prato, M. *J. Am. Chem. Soc.* **1993**, *115*, 9798–9799.
23. Wilson, S. R.; Wang, Y.; Gao, J.; Tan, X. *Tetrahedron Lett.* **1996**, *37*, 775–778.
24. Tan, X.; Schuster, D. I.; Wilson, S. R. *Tetrahedron Lett.* **1998**, *39*, 4187–4190.
25. To a solution of C_{60} (36 mg, 0.05 mmol) and D,L-alanine (9.2 mg, 0.10 mmol) in 1,2-dichlorobenzene (10 mL), acetaldehyde (11 mg, 0.25 mmol) was added and the mixture stirred at 120 °C for 20 h. The reaction process was checked by HPLC [silica gel column, solvent: benzene–EtOAc (10:1)]. The reaction mixture was purified by silica gel column chromatography (hexane–benzene–EtOAc) to give brown solid **2** (9.0 mg, 0.011 mmol, $y = 22\%$) as a *cis*- and *trans*-mixture.
26. To a solution of 4-azidobenzoic acid **3** (1.84 g, 11 mmol) in CH_2Cl_2 (5 mL), $SOCl_2$ (4.0 mL, 6.5 g, 55 mmol) in CH_2Cl_2 (5 mL) was added under argon atmosphere. Subsequently, dry DMF (1.5 mL) was added dropwise under Ar. After stirring for 2 h under Ar, the generation of acid chloride **4** was checked by TLC [solvent: hexane–EtOAc (1:1)] and then reaction mixture was filtered and concentrated in vacuo. To a solution of dimethyl fulleropyrrolidine **2** (*cis*- and *trans*-mixture, 20 mg, 0.025 mmol) in benzene (10 mL), acid chloride **4** (100 mg, 0.55 mmol) and pyridine 1 mL were added and the mixture stirred at 50 °C for 1 h. The reaction process was checked by TLC [benzene–EtOAc (1:1)], and then small amount of Et_3N was added. The products (*cis*- and *trans*-isomers) were separated by silica gel column chromatography (hexane–benzene–EtOAc) to give *cis*-**5** (8.9 mg, 9.5 μmol, $y = 38\%$) and *trans*-**5** (13.3 mg, 14.2 μmol, $y = 57\%$).
27. To a solution of 4-(3-trifluoromethylazirino)benzoic acid **6**, (9.7 mg, 0.042 mmol) with Et_3N (10 μL) in toluene (2 mL), 2,4,6-trichlorobenzoyl chloride (10 μL) was added and stirred under Ar at room temperature for 1.5 h. The reaction process was monitored by TLC [hexane–EtOAc (1:1)]. Subsequently, dimethyl fulleropyrrolidine **2** (10 mg, 12.6 μmol), DMAP 7 mg in toluene (4 mL) was added and then stirred under Ar at room temperature in dark condition for 2 days. The reaction process was monitored by TLC [benzene–EtOAc (1:1)] and then reaction mixture was purified by silica gel column chromatography (hexane–benzene–CH_2Cl_2) to give *cis*-**9** (2.5 mg, 2.5 μmol, $y = 20\%$) and *trans*-**9** (5.6 mg, 5.6 μmol, $y = 44\%$).
28. Selected spectroscopic data for *cis*-**5**: ^{1}H NMR ($CDCl_3$, 300 MHz): 2.28 (d, $J = 6.9$, 6H), 6.14 (q, $J = 6.9$, 2H), 7.23 (d, $J = 8.7$, 2H), 7.81 (d, $J = 8.7$, 2H); MALDI-TOF-MS (negative, matrix: DTT): 936 ($[M-1]^-$), 720. *trans*-**5**: 2.21(d, $J = 6.0$, 6H), 5.74 (q, $J = 6.6$, 2H), 7.22 (d, $J = 8.4$, 2H), 7.99 (d, $J = 8.4$, 2H); ^{13}C NMR ($CDCl_3$, 75 MHz): 19.9 (CH), 65.3 (CH3), 119.5 (CH), 130.2 (CH), 133.3–154.6 (C_{60}), 173.1 (CO); MALDI-TOF-MS (negative, matrix: DTT): 936 ($[M-1]^-$), 720; FT-IR (KBr): 2122 (N_3), 1670 (CO), 1600, 1260, 1182, 842, 756, 527 cm^{-1}. *cis*-**9**: ^{1}H NMR ($CDCl_3$, 300 MHz): 2.27 (d, $J = 6.7$, 6H), 6.08 (q, $J = 6.7$, 2H), 7.40 (d, $J = 8.5$, 2H), 7.81 (d, $J = 8.5$, 2H); MALDI-TOF-MS (negative, matrix: DTT): 1003 ($[M-1]^-$), 720. *trans*-**9**: 2.23 (d, $J = 6.9$, 6H), 5.17 (q, $J = 6.9$, 2H), 7.40 (d, $J = 8.3$, 2H), 7.81 (d, $J = 8.3$, 2H); MALDI-TOF-MS (negative, matrix: DTT): 1003 ($[M-1]^-$), 720.
29. Kitahara, A.; Satoh, K.; Nishimura, K.; Ishikawa, T.; Ruike, K.; Tsuda, H.; Ito, N. *Cancer Res.* **1984**, *44*, 2698–2703.
30. Satoh, K.; Hitahara, A.; Soma, Y.; Inaba, Y.; Hatayama, I.; Sato, K. *Proc. Natl. Acad. Sci. U.S.A.* **1985**, *82*, 3964–3968.

(34)

Available online at www.sciencedirect.com

SCIENCE DIRECT®

Biochemical and Biophysical Research Communications 315 (2004) 603–611

BBRC

www.elsevier.com/locate/ybbrc

A novel function of N-cadherin and Connexin43: marked enhancement of alkaline phosphatase activity in rat calvarial osteoblast exposed to sulfated hyaluronan

Misao Nagahata,[a,b,*] Toshie Tsuchiya,[b] Tatsuya Ishiguro,[a] Naoki Matsuda,[c] Yukio Nakatsuchi,[d] Akira Teramoto,[a] Akira Hachimori,[e] and Koji Abe[a]

[a] *Department of Functional Polymer Science, Faculty of Textile Science and Technology, Shinshu University, Ueda 386-8567, Japan*
[b] *Division of Medical Devices, National Institute of Health Sciences, Kamiyoga 158-8501, Japan*
[c] *Radioisotope Center, Nagasaki University, Nagasaki 852-8526, Japan*
[d] *Department of Orthopaedic Surgery, National Nagano Hospital, Ueda 386-8610, Japan*
[e] *Institute of High Polymer Research, Faculty of Textile Science and Technology, Shinshu University, Ueda 386-8567, Japan*

Received 6 January 2004

Abstract

In this study, we examined the interaction of the osteoblast which forms bone and sulfated hyaluronan (SHya). For the purpose of the creation of a new functional polysaccharide, we introduced a sulfate group in hyaluronan (Hya) of high molecular weight, and SHya of high molecular weight could be obtained for the first time. When rat calvarial osteoblast (rOB) cells were cultured with a high concentration of SHya, they formed aggregated spheroids after 4 h and the spheroids grew to about 200 μm after 24 h. We examined the expression of cell adhesion molecules in order to clarify the mechanism of aggregate formation. The N-cadherin (N-cad) and Connexin43 (Cx43) expression level of rOB cells cultured with SHya remarkably increased after 2 h. A difference in the expression of Integrin β1 (Intβ1) could not be observed between the SHya addition and control group. The alkaline phosphatase (ALPase) activity of rOB cells cultured with SHya after 8 h was significantly enhanced in comparison with control. Therefore, the sulfate group of SHya seems to enhance expression of cell adhesion protein such as N-cad and Cx43, resulting in aggregate formation and further remarkable induction of the ALPase activity of rOB cells.

Keywords: Sulfated hyaluronan; Osteoblast; Aggregation; N-cadherin; Connexin; ALPase activity

It is reported that the extracellular matrix (ECM) provides positional and environmental information essential for tissue function [1]. ECMs are complex, consisting of several different classes of molecules that may regulate modeling and remodeling [2]. Sulfated polysaccharides, such as heparan sulfate (HS) or heparin (Hep), stabilize fibroblast growth factor (FGF) and transforming growth factor β (TGF-β) in an active conformation, protect them against pH, thermal, and proteolytic degradations, and strongly potentiate their mitogenic activity in many cell types. Growth factors play a key role in the process of bone repair [3,4]. However, when the size of the defect is large, growth factor alone is not enough for bone repair. One promising way of promoting bone repair is to use cell scaffold, such as collagen [5]. However, there are problems, such as the antigenicity on the proteins. Therefore, we tried the regeneration of the bone using biocompatibility polysaccharides. Hyaluronan (Hya) has by far the highest molecular weight of the glycosaminoglycans (GAGs) and is thought to facilitate cell migration, adhesion, proliferation, and tissue repair [6].

Then, we synthesized sulfated hyaluronan (SHya) with different degrees of sulfation. We examined the effect of SHya on the cell function of rOB cells.

* Corresponding author. Fax: +81-3-3700-9196.
E-mail address: nagahata@nihs.go.jp (M. Nagahata).

0006-291X/$ - see front matter © 2004 Elsevier Inc. All rights reserved.
doi:10.1016/j.bbrc.2004.01.098

Materials and methods

Sulfated hyaluronan. On the sulfation of the polysaccharide, various methods are reported [7–10]. However, the sugar chain is easily cut off under reaction and the molecular weight lowers. Therefore, a method using sulfur trioxide (SO_3) complex was developed to prevent the lowering of the molecular weight [11–13]. The molecular weight simply lowers on Hya by acid and heating. Then, the synthesis was carried out using dimethylformamide (DMF)–SO_3 complex and trimethylamine (TMA)–SO_3 complex. Hya derivatives with different sulfation degrees can be obtained by changing the amount of DMF–SO_3 complex and TMA–SO_3 complex.

Dimethylformamide–SO_3 complex. Ten percent Hya150 (molecular weight, 1.5×10^6) solution in *N,N*-dimethylformamide (DMF) (WAKO Pure Chemical Industries) was mixed with DMF–SO_3 complex [14] and stirred for 14 h at 0 °C. The reaction mixture was then diluted, neutralized, and precipitated by adding to a large quantity of acetone. The precipitate was dissolved in distilled water again and dialyzed against distilled water.

Trimethylamine–SO_3 complex. Ten percent Hya150 solution in DMF was mixed with TMA–SO_3 complex (Aldrich Chemical) and stirred for 48 h at 60 °C. SHya was obtained after the reaction by the method equal to the above-mentioned DMF–SO_3 complex method.

The degree of substitution (DS) of SHya was 1.2, 2.1, and 3.4 as determined by the chelate titration method [15]. Moreover, the effectiveness of sulfation was also demonstrated by FT-IR analysis. The IR spectrum of SHya exhibited two absorption bands at 1240 and 820 cm^{-1} due to the S=O and SO_3^- stretching, respectively. Characteristics of SHya are summarized in Table 1 and chemical structures are illustrated in Fig. 1. The number, which is at the end of the compound's name, indicates MW [$\times 10^4$] and the subscript shows the DS.

Cell culture. The rOB cells were isolated and cultured using the method described by Hamano et al [16]. rOB cells were cultured in a sterile tissue culture dish (NUNCLON) with the use of Dulbecco's modified Eagle's medium (DMEM, Nissui-seiyaku) supplemented with 10% fetal bovin serum (FBS, Gibco). Cultures were maintained in a 5% CO_2 humidified atmosphere at 37 °C. The cells were plated in 24-well tissue culture plates (NUNCLON) or 100 mm ϕ tissue culture dish (NUNCLON) at an initial density of 5×10^4 cells/cm^2 for study of the effects of Hya and SHya on cell function. The cells were subconfluent after 2–3 days of culture and confluent after 3–4 days.

Table 1
Characteristics of polysaccharides

Polysaccharides	Number of sulfate groups per two saccharide rings	MW ($\times 10^4$)
Hya	0	30
1.2 SHya	1.2	55
2.1 SHya	2.1	20
3.4 SHya	3.4	5

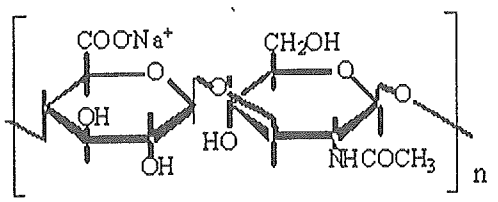

Hyaluronan (Hya)

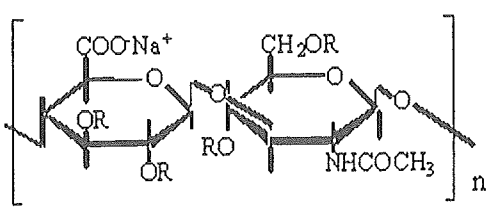

Sulfated hyaluronan (SHya)

R= SO_3Na or H

Fig. 1. Structure of hyaluronan and sulfated hyaluronan.

Western blotting analysis. Immunoblots of N-cadherin (N-cad), Integrin β1 (Intβ1), and Connexin43 (Cx43) were performed according to the method of Matsuda et al. [17]. rOB cells were plated in 100 mm ϕ dishes. The cells were incubated with SHya for different time intervals as indicated in the results, washed with phosphate-buffered saline (PBS (−)), and lysed for 30 min at 4 °C with RIPA buffer. After sonicating the lysates for 30 s using a sonicator, their protein concentrations were determined using DC protein assay (Bio-Rad Laboratories). The lysate was mixed with equal volumes of Laemmli sample buffer, and proteins were separated on 7.5% polyacrylamide gels and transferred to nitrocellulose membranes (OSMONICS). After blocking with 3% nonfat dried milk in Tris-buffered saline with Tween 20 buffer, the membranes were incubated successively with a primary antibody, followed by incubation with antimouse antibodies conjugated with ALP, and detection with ALP detection reagent (Gibco). Primary antibodies used include those recognizing N-cad, Intβ1, and Cx43. All antibodies were monoclonal mouse antibodies and were obtained from BD Transduction Laboratories.

Preparation of cell lysate for assay. Cell lysates were prepared according to the method of Hamano et al. [16]. After removal of the culture medium from the dishes, cells were washed three times with PBS (−). One milliliter of PBS (−) containing 0.04% Nonidet P-40 (Nacalai tesque) was poured into the dishes and incubated at 37 °C for 10 min. The suspension was homogenated with an ultrasonic disrupter (BH-200P, TOMY SEIKO) and centrifuged at 1000 rpm for 10 min at 4 °C. These cell lysates were used as sample solutions for the measurements of protein content and ALPase activity.

Protein content. Total protein content of cell lysate was measured by the BIO-RAD protein assay method (Protein assay, Bio-Rad Laboratories) and absorbance at 595 nm was measured using an ELISA reader (Bio-Rad Laboratories), using bovine serum albumin (WAKO Pure Chemical Industries) as reference standard.

Alkaline phosphatase activity. Alkaline phosphatase (ALPase) activity was determined by the modification of the methods of Hamano et al. [16] and Lowry et al. [18]. The reaction mixture consisted of 0.1 ml cell lysate and 0.4 ml of 16 mM *p*-nitrophenylphosphate disodium salt hexahydrate (WAKO Pure Chemical Industries). The solution was incubated at 37 °C for 30 min. The enzymatic reaction was stopped by adding 0.5 ml of 0.5 N NaOH and absorbance at 410 nm of *p*-nitrophenol liberate was measured. The enzyme activity was expressed in units/mg of protein, where 1 U corresponded to 1 nmol of *p*-nitrophenol liberate per 30 min at 37 °C. For determination of the localization of the ALPase activity, cells were rinsed with PBS (−) and fixed with 10% formalin (pH 7.4) overnight at 4 °C. These fixed dishes were rinsed three times with distilled water and Azo staining solution (5 mg naphthol AS-BI phosphoric acid sodium salt (FLUKA) in 10 ml of 0.05 M 2-amino-2-methyl-1,3-propandiol (WAKO Pure Chemical Industries) buffer (pH 9.8)) for 5 min at room temperature. Finally, they were washed three times with distilled water.

Culture conditions for estimating the interaction of serum and SHya. Four kinds of dishes were prepared as follows: (A) DMEM only, (B) DMEM with 10% FBS, (C) 2.1SHya in DMEM with 10% FBS, and (D) 2.1SHya only in DMEM into 35-mm tissue culture dish (NUNCLON), and incubated for 2 h at 37 °C, respectively. After the incubation, these dishes were washed up with PBS (−) three times. rOB cells were suspended in DMEM without serum, the cell suspensions were added into these dishes, and cell adhesion and morphological change were examined after 24 h-incubation.

Interaction of serum components and SHya. The cells were plated in serum free DMEM supplemented with fibronectin (FN), basic FGF

(bFGF), and SHya. Cells in culture were incubated at 37 °C for 24 h with 5% CO_2.

Results

Fig. 2 shows the morphologies of the attachment of rOB cells cultured with four different concentrations of 2.1SHya after 24 h. rOB cells treated with high concentrations (0.25 and 0.5 mg/ml) of 2.1SHya formed large aggregations. Western blotting was used to examine the effect of 2.1SHya on adhesion protein expression in rOB cells. The cultures were washed with cold PBS (−) and protein samples were collected by the addition of a lysis buffer. As shown in Fig. 3A, the control time-dependently increased protein levels of N-cad, Intβ1 after incubation with rOB cells for 24 h. The time-dependence of 2.1SHya stimulation of N-cad is shown in Fig. 3B. This response was considerably earlier than that observed for the control, peaking 2–6 h after 2.1SHya addition (Fig. 3C). Expression of Intβ1 was not observed in great difference for the 2.1SHya addition and control. Cx43 expression level in the 2.1SHya addition reached a peak at 2–4 h, and increase in some expression levels of protein was observed in comparison with the control (Fig. 3C). N-cadherin in Fig. 4 shows the morphologies of the attachment of rOB cells treated with different DS SHya and Hya after 24 h. Cell aggregations were formed in the case of high DS SHya (2.1SHya, 3.4SHya). In the meantime, with low DS 1.2SHya or nonsulfated Hya, aggregations were not formed. However, when 1.2SHya was added in high density, rOB formed aggregations. Fig. 5 shows rOB cell proliferation in the presence of SHya and Hya. In the presence of 2.1SHya, cell proliferation was suppressed after seeding 48 h. However, rOB cells treated with 2.1SHya gradually proliferated afterwards and it reached confluence after 120 h. Hya showed similar trends in the control (TCD). Fig. 6 shows photographs of the Azo staining used for the determination of ALPase activity localization on rOB cell monolayers and aggregates cultured for 24 h. The staining also immaturely dyed the central part of the aggregation observed in the 2.1SHya. The rOB cells in TCD and Hya did not stain with Azo staining. The ALPase activity was only expressed in the aggregates. Compared with the control and Hya, 2.1SHya also time-dependently enhanced the ALPase activity of rOB cells when examined at a concentration of 0.5 mg/ml (Fig. 7). The effect of the existence of serum component and 2.1SHya on the formation of aggregation of rOB cells was examined (Fig. 8). rOB cells did not form aggregations without 2.1SHya in the case of the serum-free medium (Fig. 8D). The adherent cell number increased when it

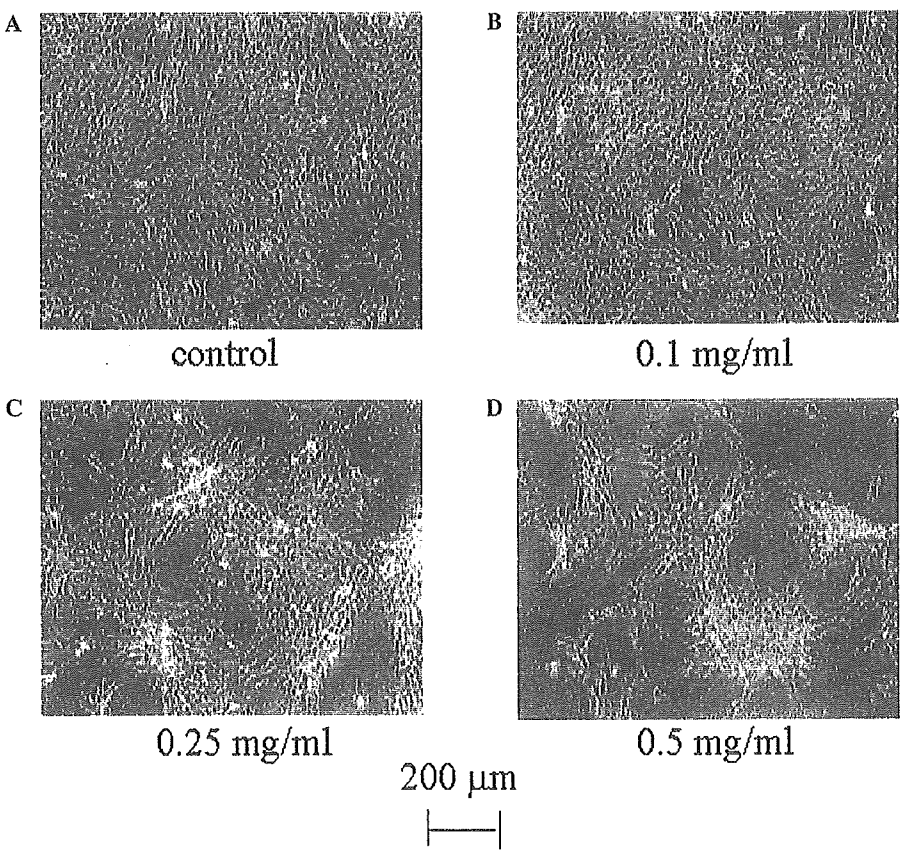

Fig. 2. Relationship between 2.1SHya concentration and rOB cell adhesion after 24 h. rOB cells were treated with various concentrations of 2.1SHya. (A) Control. (B) 0.1 mg/ml of 2.1SHya. (C) 0.25 mg/ml of 2.1SHya. (D) 0.5 mg/ml of 2.1SHya. Phase contrast micrographs. Scale bar 200 μm.

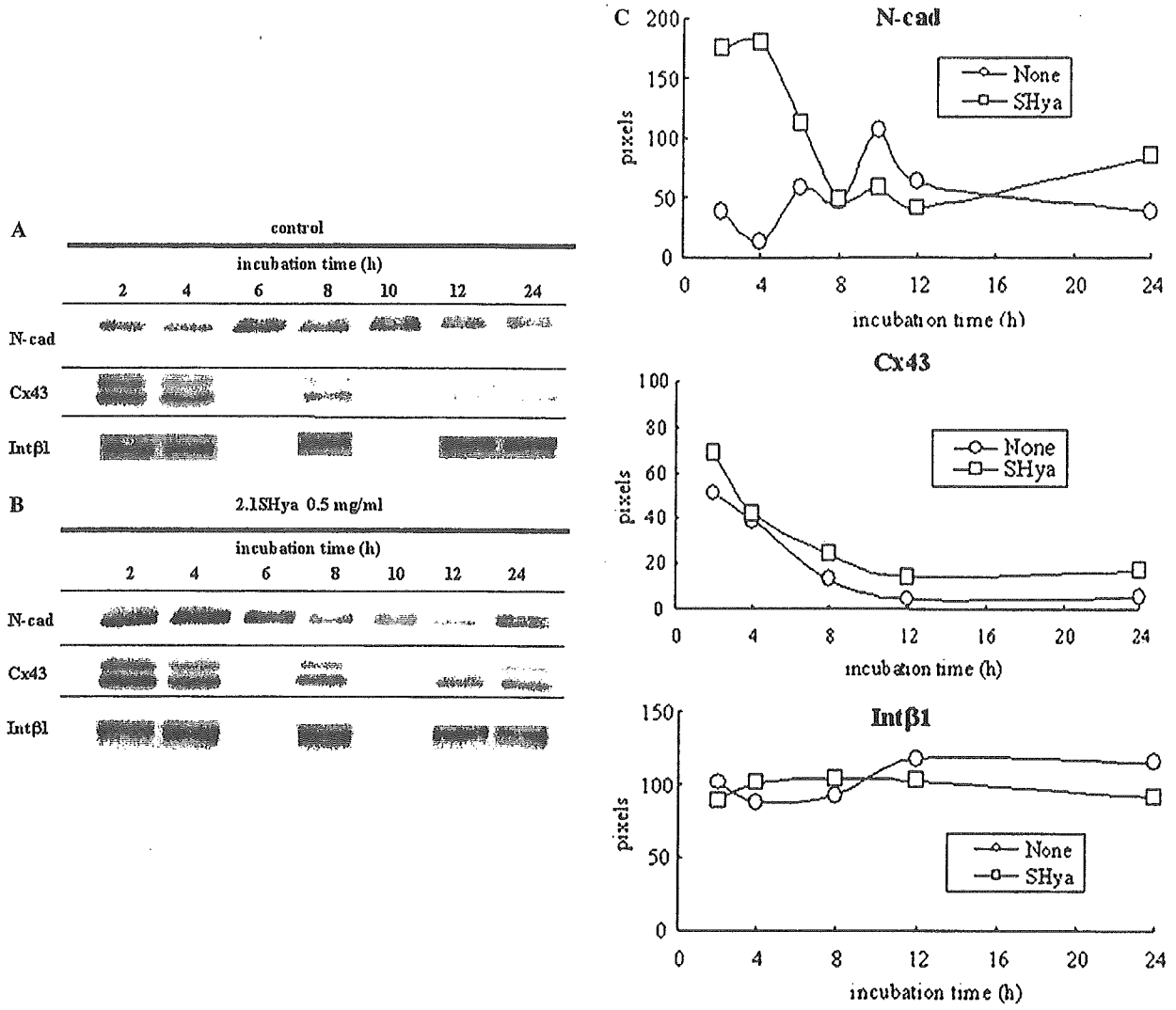

Fig. 3. Effect of SHya on adhesion protein expression in rOB cells. rOB cells were incubated with 2.1SHya for the times shown. Cells were lysed and proteins were separated by SDS–PAGE followed by Western blotting. (A) Without 2.1SHya (B) with 2.1SHya (C) quantification of band intensities was measured by NIH images.

was incubated in the culture medium including the serum (Fig. 8B) in comparison with the serum-free system. However, when SHya coexisted with the serum, rOB cells formed aggregations (Fig. 8C). rOB cells were seeded onto the plates in the presence or absence of FN and bFGF of added SHya for the study of effects of serum protein and SHya on cell aggregation (Fig. 9). bFGF was shown to form aggregation in rOB cells but not in the case of FN addition. Furthermore, when SHya was added with the bFGF, the cell aggregation was increased by the addition of SHya under the presence of bFGF.

Discussion

The aim of this study was to elucidate the mechanism of the enhancement of ALPase activity induced by the high molecular weight of sulfated polysaccharides. Hep, HS, and Hya are common components of the ECM in most tissues [19]. It is reported that sulfated polysaccharides like Hep/HS are the major FGF, TGF-β, and bone morphogenetic protein (BMP)-binding molecules in the ECM [20]. However, the molecular weights of Hep/HS and chondroitin sulfate (Chs) are lower than Hya [21]. Therefore, we synthesized SHya with varying DS and high molecular weight in order to obtain a high molecular weight of sulfated polysaccharides. Hya is easily decomposed in heat and acid [19]. Therefore, by the change of type and quantity of the SO_3 complex, SHya of varying DS and high molecular weight was synthesized. In this study, we examined the effect of SHya on the initial differentiation marker of the osteoblast. As a result of examining the effect of SHya in rOB cells on cell morphology, the following fact became clear: rOB cells formed aggregations in over 3 mg/ml

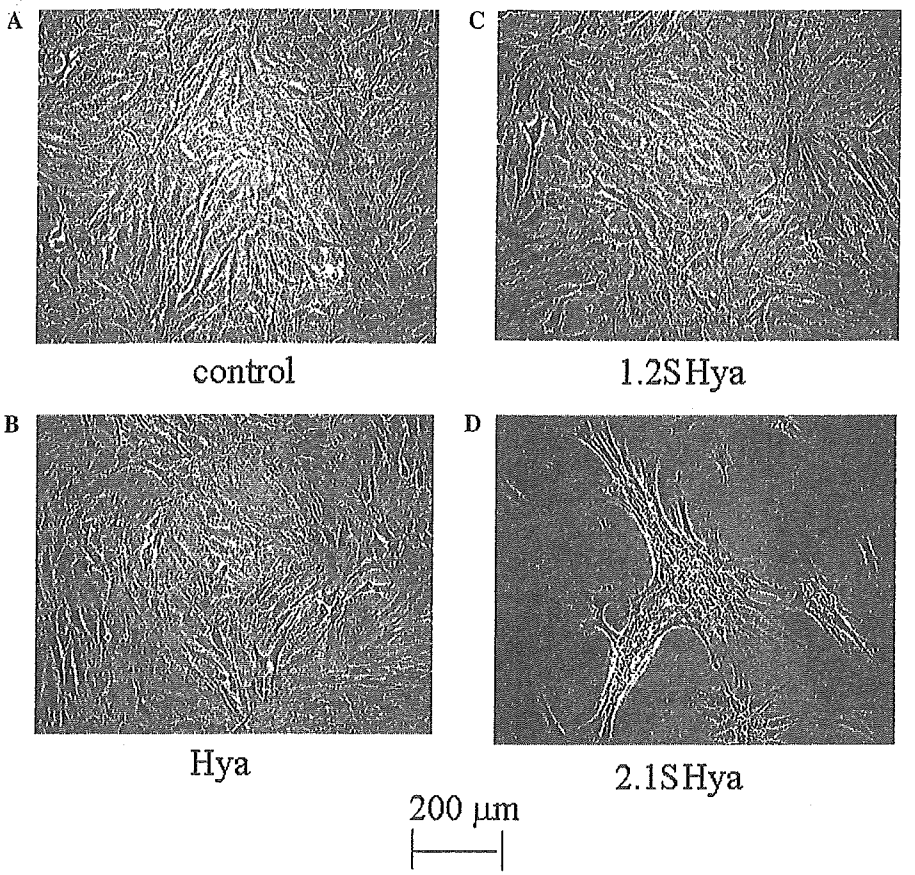

Fig. 4. Cell morphologies of rOB cells in the presence of 0.5 mg/ml Hya and SHya after 24 h. rOB cells were treated with Hya and varying DS of SHya. (A) Control, (B) Hya, (C) 1.2SHya, and (D) 3.4SHya.

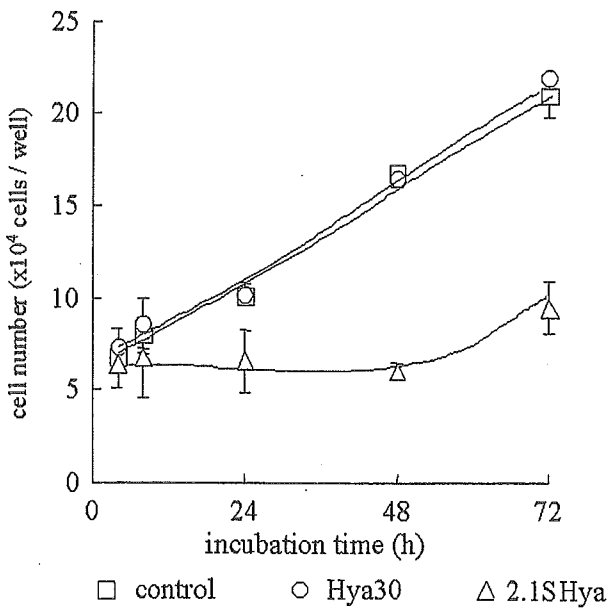

Fig. 5. Effect of 0.5 mg/ml Hya and SHya on the proliferation of rOB cells. rOB cells were treated with Hya and 2.1SHya for 72 h. The proliferation of rOB cells treated with Hya and 2.1SHya was determined. Values are means ± SD for four dishes.

concentration in the case of SHya of low DS (1.2SHya) and in over 0.25 mg/ml concentration in the case of SHya of high DS (2.1SHya, 3.4SHya). However, rOB cells cultured with Hya without the sulfate group did not form aggregations (data not shown). Also, aggregations were not formed when Hep and Chs were added. After the SHya addition, rOB cells began to form aggregations after 4 h and large aggregations were formed after 24 h. Therefore, by introducing a sulfate group into the hyaluronan, rOB cells formed aggregations.

Cell–cell contacts and communication between bone cells are essential for coordinated bone development and remodeling. Cell–cell adhesion mediated by the cadherin superfamily plays an important role in osteogenesis. Cadherins play essential roles in the regulation of several physiological processes such as cell migration, proliferation, and differentiation [22]. Tsutsumimoto et al. [23] reported that the expression of N-cad is involved in the aggregate formation of MC3T3-E1. Also, integrins are the principle mediators of the molecular dialogue between a cell and its ECM environment such as collagen and fibronectin [24,25]. Osteoblasts express several integrin subunits and their presence may be important in

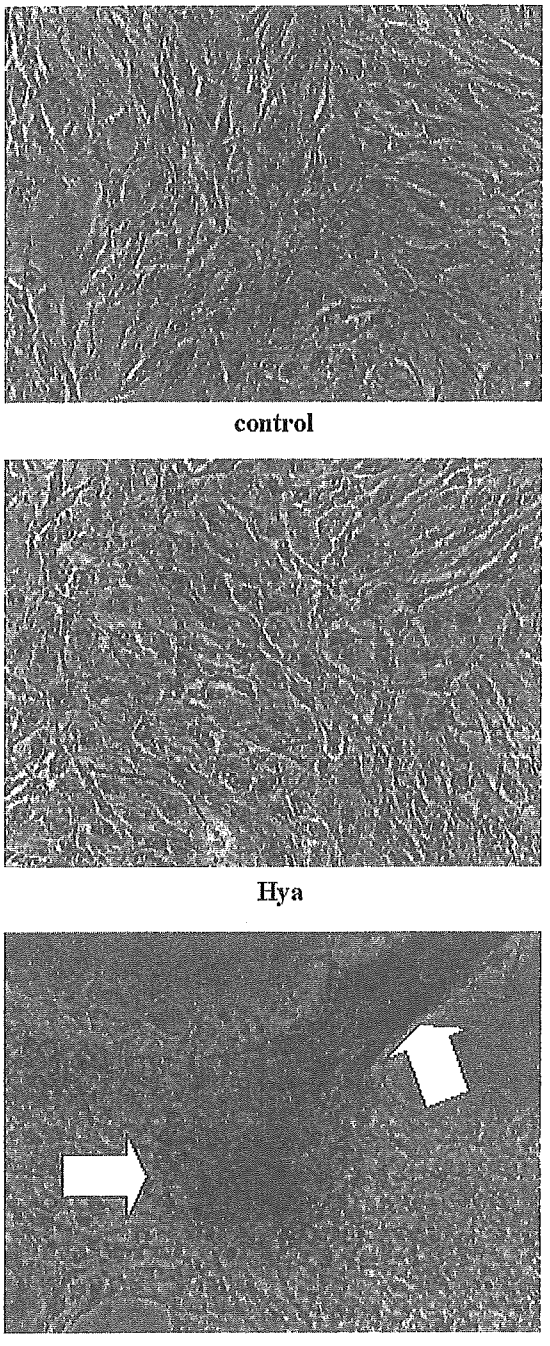

Fig. 6. Appearance of Azo-stained cultures of rOB cells in the presence of 0.5 mg/ml Hya and SHya after 24 h. rOB cells were treated with Hya and 2.1SHya for 24 h. rOB cells were stained by the Azo stain method.

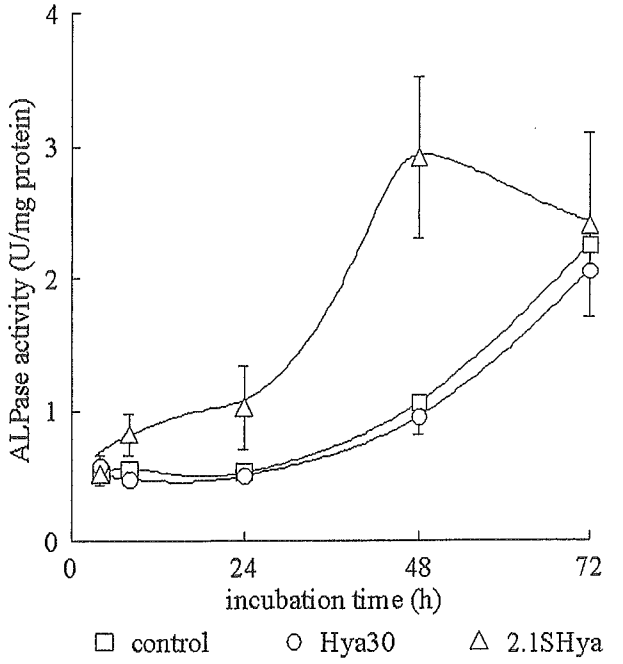

Fig. 7. Effect of 0.5 mg/ml Hya and SHya on the ALPase activity of rOB cells. rOB cells were treated with Hya and 2.1SHya for 72 h. The ALPase activity of rOB cells treated with Hya and 2.1SHya was determined. Values are means ± SD for four dishes.

regulating the response of these cells to the ECM, suggesting that integrin participates in the differentiation. By Western blotting, the expression of N-cad and Intβ1 proteins in osteoblasts was confirmed. In the presence of 2.1SHya, rOB cells increased protein levels of N-cad at early stages, but protein levels of Intβ1 were not observed in great difference between the 2.1SHya addition and control group. To clarify the roles of N-cad in SHya-induced cell aggregation, the effects of N-cad function-perturbing agents such as blocking antibodies were tested. This N-cad antibody was shown to inhibit cell–cell aggregation in rOB cells. These results confirm a direct involvement of N-cad in aggregation process (data not shown). Gap and adherens junctions are observed in osteoblast cell–cell contact [26,27]. Gap junctional intercellular communication (GJIC) is the key function by which cells exchange small molecules including signal molecules directly from the inside of a cell to neighboring cells. Gap junctions that are mediated by Cx have been well studied in osteoblasts. Among the Cx family, Cx43 is a major protein in osteoblasts [28]. By Western blotting, the expression of the Cx43 protein in these cells was confirmed. Cx43 expression level in the 2.1SHya addition reached a peak at 2–4 h, and the increase in expression level of protein was observed in comparison with the control. Some reports have proposed that cadherin is also involved in the regulation of the GJIC. This suggests that cadherin-mediated cell–cell adhesion is essential for GJIC and cadherin may also regulate GJIC in osteoblasts. Chiba et al. [29] demonstrated that Cx43 expression parallels ALPase activity and osteocalcin secretion in differentiating human osteoblastic cells. These data suggest that Cx43 expression contributes to osteoblastic differentiation.

Proliferation of rOB cells after aggregation formation was inhibited with the SHya addition more than with